Insights on cellulose hydrolysis in the porous structure of biomass particles using the lattice Boltzmann method

Haoyang Wei[1,2], Xiangqian Wei[1,2], Siwei Liu[2], Weitao Sun[1,2], Yunlong Tu[1,2], Chengguang Wang[2] ✉,
and Longlong Ma[1,3] ✉

[1]Department of Thermal Science and Energy Engineering, University of Science and Technology of China, Hefei 230027, China;
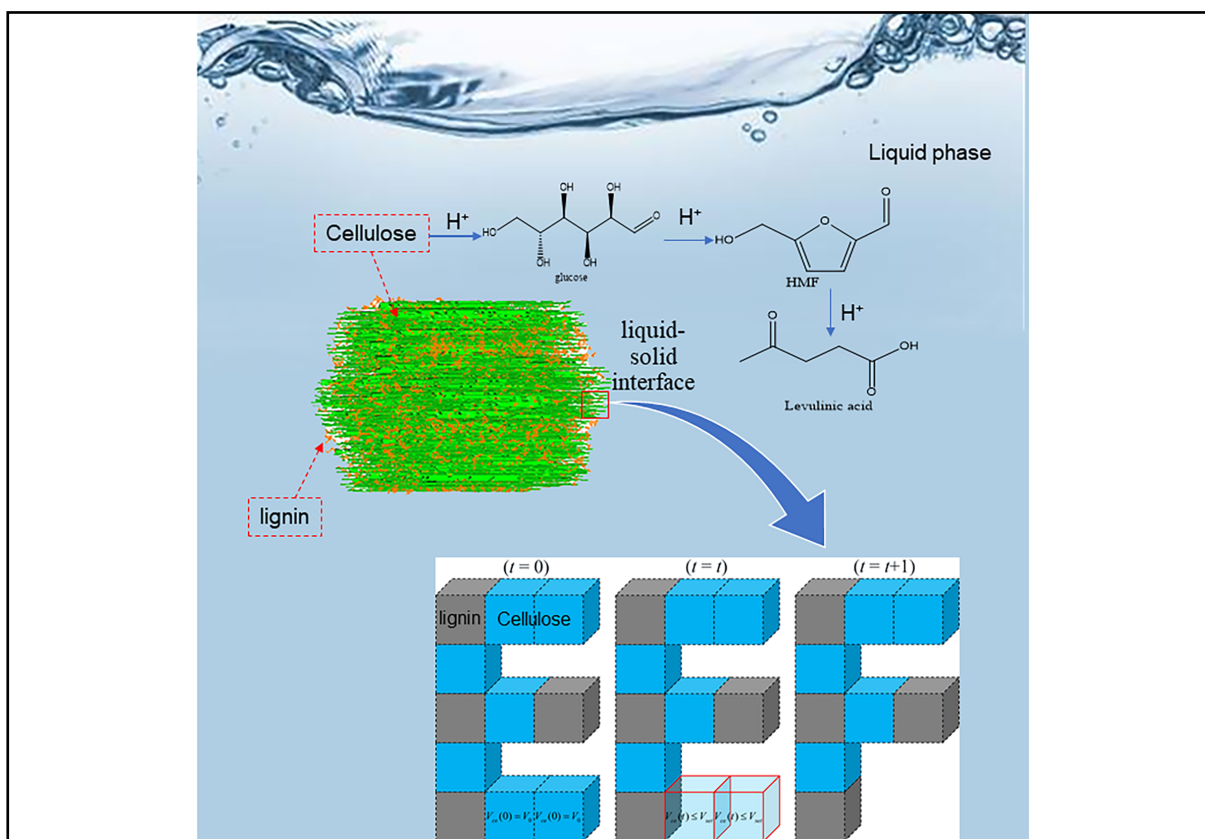[2]CAS Key Laboratory of Renewable Energy, Guangzhou Institute of Energy Conversion, Chinese Academy of Sciences, Guangzhou 510640, China;
[3]Key Laboratory of Energy Thermal Conversion and Control of Ministry of Education, School of Energy and Environment, Southeast University, Nanjing 210096, China

✉Correspondence: Chengguang Wang, E-mail: wangcg@ms.giec.ac.cn; Longlong Ma, E-mail: mall@seu.edu.cn

Graphical abstract

Schematic diagram of the hydrolysis of lignocellulose biomass solid residues to levulinic acid (LA) and solid-liquid dissolution.

Public summary

- In order to explore the reaction and transport inside the porous biomass solid residue, based on the lattice Boltzmann method, a numerical model coupling physicochemical processes was established.

- By changing the reaction parameters, the optimal reaction conditions under different working conditions were explored.

Insights on cellulose hydrolysis in the porous structure of biomass particles using the lattice Boltzmann method

Haoyang Wei[1,2], Xiangqian Wei[1,2], Siwei Liu[2], Weitao Sun[1,2], Yunlong Tu[1,2], Chengguang Wang[2] ✉,
and Longlong Ma[1,3] ✉

[1]Department of Thermal Science and Energy Engineering, University of Science and Technology of China, Hefei 230027, China;
[2]CAS Key Laboratory of Renewable Energy, Guangzhou Institute of Energy Conversion, Chinese Academy of Sciences, Guangzhou 510640, China;
[3]Key Laboratory of Energy Thermal Conversion and Control of Ministry of Education, School of Energy and Environment, Southeast University, Nanjing 210096, China

✉Correspondence: Chengguang Wang, E-mail: wangcg@ms.giec.ac.cn; Longlong Ma, E-mail: mall@seu.edu.cn

Abstract: Lignocellulose biomass has been recognized as one of the most promising sources of low-cost and renewable biofuels, and its conversion into alternative fuels and valuable platform molecules has attracted widespread attention. The porous solid residue from lignocellulose biomass, which was pretreated by steam-stripping, is catalyzed by dilute sulfuric acid to form levulinic acid (LA). The process includes porous media diffusion, multicomponent reactive transport, liquid-solid interface reaction, and cellulose dissolution. Understanding the interactions between these complex physicochemical processes is the basis for optimizing the performance of the hydrolysis reaction. In this study, a porous reaction transport model based on the lattice Boltzmann method (LBM) was established to simulate the conversion of cellulose to LA which was catalyzed by dilute acid. The simulation results were compared with the existing experimental results to verify the accuracy of the model. The simulation results showed that temperature has a significant effect on hydrolysis and the highest carbon yield was obtained at 180 °C. Without considering the lignin reaction, the higher the sulfuric acid concentration, the better is the hydrolysis efficiency in the range of 4% − 8%. The influence of cellulose content and steam-stripping the residue porosity on the dissolution rate of cellulose was also evaluated. The average dissolution rate of cellulose is the highest within 75 min, when the porosity is 0.7 and the cellulose content is 50%.

Keywords: lattice Boltzmann method; multiphase reactive transport; porous media structure; cellulose dissolution

CLC number: TQ352   **Document code:** A

1 Introduction

The massive consumption of fossil resources exacerbates environmental problems, whereas biomass energy conforms with carbon neutralization and environmental protection strategies. Lignocellulose biomass has been recognized as a promising low-cost and renewable biofuel, and its conversion into alternative fuels and valuable platform molecules has attracted widespread attention[1−5]. One of the important platform molecules, levulinic acid (LA), can be used as a fuel additive, polymer precursor, and resin precursor. Many studies have reported the properties and potential industrial applications of LA and its derivatives[6,7].

The extraction of LA from lignocellulose is technically challenging due to the complex composition of lignocellulose raw materials, including cellulose, lignin, and hemicellulose. Cellulose is the key raw material for the extraction of LA. The process of LA extraction from lignocellulose biomass has multiple steps, including pretreatment, hydrolysis, dehydration, and rehydration[8]. After the steam-stripping pretreatment of biomass raw materials, the hemicellulose is re-

moved[9,10]. The remaining solid residue is composed of cellulose and lignin and a porous medium, which improves the reaction efficiency of the subsequent hydrolysis of cellulose[11,12].

Two different methods are usually used for the acid-catalyzed hydrolysis of cellulose. The first uses a high concentration of inorganic acid as the catalyst[13] and has a low operating temperature (20 − 50 °C), but a high catalyst recovery cost. The second uses a dilute acid catalyst at high temperatures (170 − 240 °C). This method is low cost and a common method for cellulose hydrolysis[14−16]. During the hydrolysis process, the conversion of cellulose to LA is catalyzed by dilute acid solution at high temperature and two main factors affect the LA yield: (i) the process operation parameters (e.g., different temperature, dilute acid concentration, and cellulose content) which significantly affect the reaction performance of cellulose hydrolysis[16]; and (ii) the reaction by-products are surrounded by the formation of humins which reduces the selectivity of LA[17,18].

The process of extracting LA from lignocellulose biomass is shown in Scheme 1. The hydrolysis process of cellulose in solid residue includes complex physicochemical phenomena
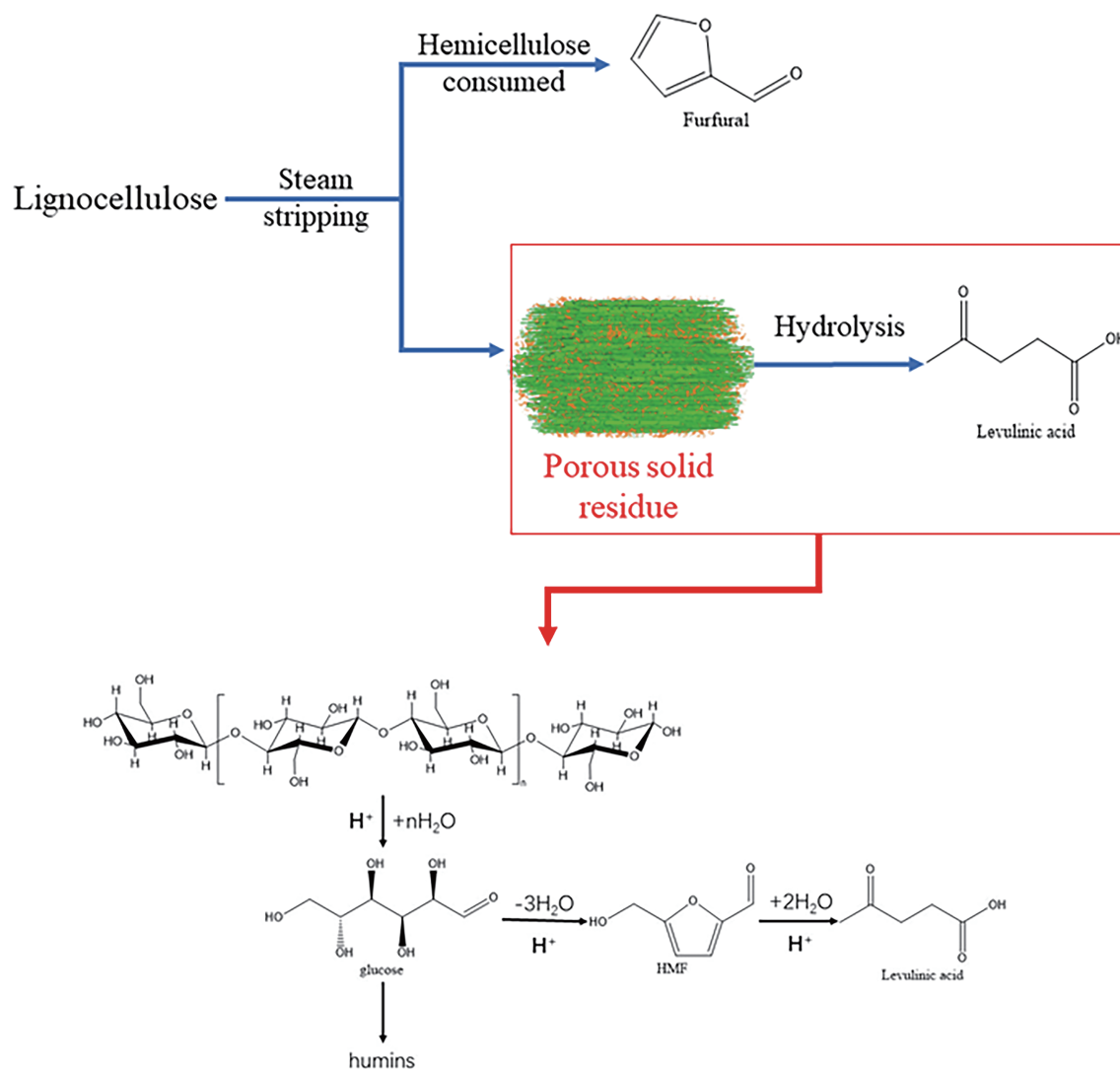
Scheme 1 Technological process for the preparation of levulinic acid (LA) from lignocellulose.

which have a significant effect on the performance of the cellulose hydrolysis, such as transport problems in porous media, multicomponent mass transfer, liquid-solid interface reaction, and dissolution of cellulose. Investigating and understanding the influence mechanism of these physicochemical processes is crucial for reaction optimization. However, due to the complexity of the reactive-transport process in porous media, the coupling mechanisms are difficult to obtain through experimental study alone. Therefore, in this study, we developed a numerical model for the simulation of the hydrolysis process of cellulose in solid residues which may elucidate the interactions of various physicochemical sub-processes involved in the reaction system.

Computational fluid dynamics (CFD) methods are powerful tools to study complex multiphase fluid flow and chemical reactions and provide insights for optimizing reactor operating conditions. Among the various CFD methods, the lattice Boltzmann method (LBM) is a mesoscopic numerical algorithm based on the Boltzmann transport equation, which plays an important role in multi-scale and multiphase flow simulation. In recent years, it has developed into a reliable and efficient numerical simulation method[19–21]. LBM is widely used to study a variety of physical and chemical phenomena, such as heat transfer[22], phase transition[23, 24], transport in porous media[25, 26], and heterogeneous catalysis[27]. LBM has distinct advantages in the numerical simulation of multiphase reaction flow and interface dynamics of complex pore-scale systems because of its efficiency for modeling the transport process of various complex structures and the relatively simple program implementation[28].

Among the LBM models related to multiphase flow, the Shan-Chen (SC) pseudopotential model[29] has been widely used because of its simplicity and efficiency. Pan et al.[30] used the SC model to simulate two-phase flow in porous media and obtained results which were consistent with the experimental data. Mei et al.[31] used the SC model to simulate the reaction and mass transfer process in a liquid membrane catalytic reactor. In recent years, many studies have proposed improved models of the SC model, including models coupled with non-ideal equations of state such as the Carnahan-Starling equation[32, 33], models using the multi-relaxation time (MRT) scheme, or the Bhatnagar-Gross-Krook (BGK) approximation[34]. While efforts have been made to introduce CFD technology into related chemical industries, the applica-

tion of LBM in heterogeneous catalysis of lignocellulose biomass and its derivatives has rarely been reported. Few studies have focused on the hydrothermal catalytic conversion of biomass and its derivatives[28, 31, 33].

Constructing a reasonable numerical model to study the interaction of complex physicochemical processes in the hydrolysis of solid residues still presents various challenges. The reaction systems in the existing models are also quite different from the models required for catalytic conversion of biomass. The purpose of this study was to establish a multiphase reactive transport model in porous media and then simulate the process of hydrolysis of pretreated solid residues to LA. The model considers the multi-component transport of porous solid residue, the dissolution of cellulose at the solid-liquid interface, and heterogeneous catalytic reactions. The quartet structure generation set (QSGS)[35] was used to construct the porous structure of the solid residue pretreated by steam-stripping. The effects of different temperatures and acid concentrations on the hydrolysis reaction were investigated, and the response of the hydrolysis performance to the porosity of the solid residues were analyzed. The influence of the proportion of cellulose in the solid residue on the hydrolysis performance was also evaluated and based on the results, improvement strategies for reactor performance have been proposed.

2 Model framework

2.1 Catalytic reactions model

Lopes et al.[36] established a kinetic model for the conversion of cellulose to LA catalyzed by dilute acid. After the steam-stripping pretreatment, the hemicellulose in the biomass was removed, and the solid residue mainly consisted of cellulose and lignin. During hydrolysis, due to the low reactivity of lignin in dilute acid catalysis, the hydrolysis of lignin can be ignored[10]. The physicochemical processes of hydrolysis include the following: (i) cellulose is broken down into smaller fragments and then converted into glucose; (ii) glucose is isomerized to fructose and further dehydrated to form 5-hydroxymethylfurfural (HMF), in which parts of the glucose are converted to humins; (iii) HMF is rehydrated to form LA and formic acid (FA). The reaction kinetic models are as follows:

Cellulose dissolution:

$$\frac{d[\text{cellulose}]}{dt} = -k_1[\text{cellulose}]. \tag{1}$$

Glucose dehydration:

$$\frac{d[\text{glucose}]}{dt} = k_1[\text{cellulose}] - k_2[\text{glucose}] - k_3[\text{glucose}]. \tag{2}$$

Reaction of HMF:

$$\frac{d[\text{HMF}]}{dt} = k_2[\text{glucose}] - k_4[\text{HMF}]. \tag{3}$$

Side reaction:

$$\frac{d[\text{humins}]}{dt} = k_3[\text{glucose}]. \tag{4}$$

Generation of LA：

$$\frac{d[\text{LA}]}{dt} = k_4[\text{HMF}]. \tag{5}$$

The specific reaction rate constant is obtained from the Arrhenius formula:

$$k = A\exp\left(-\frac{E_a}{RT}\right). \tag{6}$$

The Arrhenius formula was modified based on a previous study of the hydrogen ion catalytic reaction mechanism in cellulose acid hydrolysis[36]. Thereafter, the numerical model of the coupling acid concentration influence mechanism is constructed:

$$k_i = A_i\exp\left(-\frac{E_{Ai}}{RT}\right)(C_{\text{H}^+})^{m_i}, \tag{7}$$

where A_i (min^{-1}) is the frequency factor, E_{Ai} is the activation energy (kJ·mol^{-1}), m_i is the reaction order of the concentration of hydrated hydrogen ions, T is the temperature (K), C_{H^+} is the concentration of H_2SO_4, and R is the ideal gas constant. The reaction kinetic model parameters used in the experimental study were based on Ref. [36] and are listed in Table 1.

2.2 3D geometric model

For the construction of the model and the simulations of fluid reaction, mass transfer, and phase transition, the following assumptions are made:

(i) The hemicellulose is removed during the pretreatment process[9] and due to the low acid concentration and non-reaction of lignin, the humin does not form a solid residue during hydrolysis[10].

(ii) The two components (cellulose and lignin) are all regarded as impermeable solids, and the full bounce boundary scheme is adopted.

(iii) The physical parameters remain unchanged during the reaction.

(iv) Only diffusion is considered in this single particle model study which focuses on the internal transport reaction

Table 1. Variables of the reaction kinetic model and simulations[36].

Parameters	Values	Description
A_{CEL} (min^{-1})	1.12×10^5	Frequency factor of converting cellulose
A_{GLC1} (min^{-1})	4.50×10^5	Frequency factor of glucose to HMF
A_{GLC2} (min^{-1})	4.01×10^4	Frequency factor of glucose to humins
A_{HMF} (min^{-1})	3.18×10^5	Frequency factor of converting 5-HMF
E_{CEL} (kJ·mol^{-1})	57.5	Activation energy of converting cellulose
E_{GLC1} (kJ·mol^{-1})	32.54	Activation energy of glucose to HMF
E_{GLC2} (kJ·mol^{-1})	37.6	Activation energy of glucose to humins
E_{HMF} (kJ·mol^{-1})	24.42	Activation energy of converting HMF
m_{CEL}	0.31	Hydrogen ion order of cellulose
m_{GLC1}	2.3	Hydrogen ion order of glucose to HMF
m_{GLC2}	1.084	Hydrogen ion order of glucose to humins
m_{HMF}	1.94	Hydrogen ion order of HMF
R (J·mol^{-1}·K^{-1})	8.31	Gas constant
Δx	3.75×10^{-5}	Grid step
Δt	4.45×10^{-2}	Time step

process of porous residues.

Since most of the hemicellulose is removed from the lignocellulose, the geometric model mainly contains cellulose and lignin. In lignocellulose, the cellulose is mainly in the shape of tube bundles, while the lignin is disordered and reticulate. The geometric model was generated by QSGS[37, 38]. First, the growth nuclei of the cellulose were randomly generated in the cylindrical space and therefore the growth probabilities in all directions were adjusted to produce cellulose with a regular arrangement of tube bundles. Second, the growth nuclei of lignin in the cylinder space were randomly arranged based on the generated cellulose, and the growth probabilities in all directions were adjusted to form irregular lignin fragments. The green in Fig. 1 is cellulose and the orange is lignin.
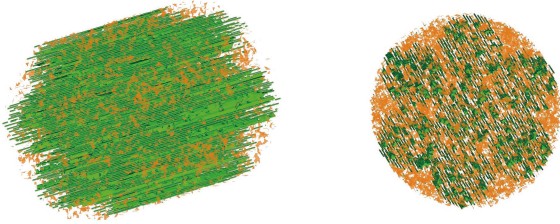

Fig. 1. Residue structure generated by the program .The green part is cellulose, the yellow part is lignin.

2.3 Multiphase lattice Boltzmann method (LBM)

The LBM can be divided into two parts. The first step is collision, which updates the density distributions according to the equilibrium distribution function. The second step is the streaming of the distributions toward the neighbor nodes. In this study, the simulation region was discretized into nodes. To simulate the coupling of reactive transport and multiphase fluid flow in the LBM, we used the lattice Bhatnagar-Gross-Krook (LBGK) model as the discrete approximation of the Boltzmann equation. In the LBGK model, the fluid discrete distribution function g was introduced, the D3Q19 discrete velocity model was adopted, and the evolution equation is expressed as:

$$g_{i,k}(\boldsymbol{x}+e_i\Delta t, t+\Delta t)-g_{i,k}(\boldsymbol{x},t)=-\tau_{D,k}^{-1}\left[g_{i,k}(\boldsymbol{x},t)-g_{i,k}^{eq}(\boldsymbol{x},t)\right]+\omega_{i,k}S_k\Delta t, \tag{8}$$

where $g_{i,k}$ is the concentration distribution function of the k component at site x and time t. $\tau_{D,k}^{-1}$ is the dimensionless relaxation time of mass transfer, and S_k is the source term of the catalytic reaction. Δt and $\omega_{i,k}$ are the time step and the weight factor, respectively. The corresponding equilibrium distribution is expressed as:

$$g_{i,k}^{eq}(\boldsymbol{x},t)=\omega_{i,k}C_k(\boldsymbol{x},t)\left[1+\frac{\boldsymbol{e}_i\cdot\boldsymbol{u}^{eq}}{c_s^2}+\frac{(\boldsymbol{e}_i\cdot\boldsymbol{u}^{eq})^2}{2c_s^4}-\frac{(\boldsymbol{u}^{eq})^2}{2c_s^4}\right]. \tag{9}$$

The weight factor (ω_i) corresponding to the D3Q19 model is expressed as:

$$\omega_i=\begin{cases}\frac{1}{3},i=0;\\\frac{1}{18},i=1-6;\\\frac{1}{36},i=7-18.\end{cases} \tag{10}$$

The lattice sound speed equation is:

$$c_s=\Delta x/\left(\sqrt{3}\Delta t\right), \tag{11}$$

where Δx is the lattice spacing. The concentration and source terms are obtained by the following equations:

$$C_k(\boldsymbol{x},t)=\sum_{i=0}^{18}g_{i,k}(\boldsymbol{x},t), \tag{12}$$

$$S=\sum_n k_nC_n. \tag{13}$$

k_n is the kinetic parameter of the reaction and C_n is the concentration of the substrate. The macroscopic governing equation of the concentration is:

$$\frac{\partial C_k}{\partial t}+\nabla\cdot(C_k\boldsymbol{u})=D\nabla^2C_k. \tag{14}$$

2.4 Dissolution model

Solid cellulose dissolves to form glucose, and the glucose reacts in the dissolved liquid phase and therefore, building a suitable dissolution model is necessary. The volume of pixels (VOP) method, introduced by Chen et al.[39, 40], is widely used and can solve most phase transition problems. Liu et al.[28] successfully used the VOP method to simulate the coking process which involves the catalytic conversion of glucose to LA. Chen et al.[41] studied the polyreactive migration in CO_2 dissolution and trapping using the VOP method. At each time step, at the solid-liquid interface of the reaction, the volume of the solid node V_s is updated according to Chen et al.[40]:

$$\frac{\partial V_s}{\partial t}=\pm A_rV_mk_iC_i, \tag{15}$$

where V_m is the molar volume and A_r is the specific surface area.

Using the VOP method, the dimensionless solid volume V_s of a node represents its ability to become a solid node at that time. When the solid dissolves, the right side of Eq. (14) is negative, but when the liquid product condenses, it becomes positive. At the end of each iteration, if V_s reaches 0, the node changes from a solid state to a flow state. If V_s reaches a critical value, a random fluid node near this node changes from a flow state to a solid state.

For this model of cellulose hydrolysis, the solid form is not considered, and the V_s decreases continuously during the cellulose hydrolysis. In each time step, the V_s of the corresponding cellulose solid node will decrease if dissolution occurs at this node. When V_s is reduced to 0 or less than the set value, the solid node will be converted into a fluid node. The movement of the solid-liquid interface is shown in Fig. 2.

By substituting Eq. (7) into Eq. (14), Eq. (16) is derived:

$$\frac{\partial V_s}{\partial t}=-A_rV_mA_1\exp\left(-\frac{E_{a1}}{RT}\right)C_{H^+}^{m_1}C_i. \tag{16}$$

From this, it can be inferred that:

$$V_s(t+\Delta t) = V_s(t) - A_r V_m A_1 \exp\left(-\frac{E_{a1}}{RT}\right) C_{H^+}^{m_1} C_i. \quad (17)$$

Since cellulose is solid, its initial concentration cannot be obtained directly. In this study, the initial dimensionless solid volume of each cellulose node is V_0, and the mass of cellulose in each node is:

$$\text{mass}_{CEL} = k * V_0 * \rho. \quad (18)$$

The initial concentration of cellulose can be expressed as:

$$C_{CEL,0} = \frac{k * V_0 * \rho}{M_{CEL} * V_{reaction}}, \quad (19)$$

$$\rho(\boldsymbol{x},t) = (1+\delta)\rho(\boldsymbol{x},t-\Delta t)\frac{\sum \rho(\boldsymbol{x},t-\Delta t)}{\sum_1^m \rho_{new}(\boldsymbol{x},t) + \sum \rho(\boldsymbol{x},t-\Delta t) - \sum_1^n \rho_{old}(\boldsymbol{x},t-\Delta t)}, \quad (20)$$

where δ is a random perturbation to achieve phase transition, $\sum \rho(\boldsymbol{x},t-\Delta t)$ is the total density of the system at time $t-\Delta t$, and $\sum_1^m \rho_{new}(\boldsymbol{x},t)$ and $\sum_1^n \rho_{new}(\boldsymbol{x},t-\Delta t)$ are the densities of new liquid nodes and old solid nodes, respectively. Eq. (20) and the hypothesis indicate that the velocity of the newly generated liquid node is zero. This leads to zero momentum, does not add additional momentum to the system and ensures the conservation of mass and momentum in the system.

3 Results and discussion

3.1 Model verification

The simulation results were compared with experimental results of cellulose hydrolysis from Ref. [36] to verify the accuracy and reliability of the present model. Previous studies assessed that the concentration changes of glucose, HMF, and LA during cellulose hydrolysis occur at $150-190$ °C temperatures and $3\%-7\%$ acid concentration. The relevant parameters are shown in more detail in Table 1. The dimensionless concentration is defined as:

where M_{cel} is the molar mass of cellulose and $V_{reaction}$ is the volume of the reaction.

Managing the flow and concentration information of these nodes is challenging. The conservation of mass, momentum, and species in the system should be guaranteed when the reaction-generated water is sufficient to change a solid node into liquid node. Chen et al.[39] provided a phase change boundary treatment that ensured the mass and momentum conservation of the system and the convergence of the simulation. The ρ_{new} which represents the density of the new liquid node, is the averaged density of the nearest-neighbor liquid nodes. The density of each fluid node is modified by:

$$C_i(t) = \iiint_{V_{re}} C_i(x,t) dV / \iiint_{V_{re}} C_0 dV, \quad (21)$$

where $C_i(t)$ is the dimensionless concentration of component i at t time, and V_{re} is the reaction volume.

Figs. 3, 4, and 5 show that the dimensionless concentration of glucose, HMF, and LA varied with reaction time under different conditions. The evolution curve of the concentration of each component with the reaction time predicted by the model showed correlation with the results indicated in the literature, which demonstrated the accuracy and reliability of the model used in our study. The experimental results were derived from Lopes et al.[36].

3.2 Effect of temperature

Previous studies[18,42] have shown that when acid catalyzes the conversion of cellulose to LA in the γ-Valerolactone/H_2O biphasic solvent system, the LA yield increases when the temperature reaches 160 °C, but decreased rapidly when the temperature exceeds 240 °C. This is likely due to the decomposition of LA into by-products at higher temperatures[43]. However, when acid catalyzes the conversion of cellulose to
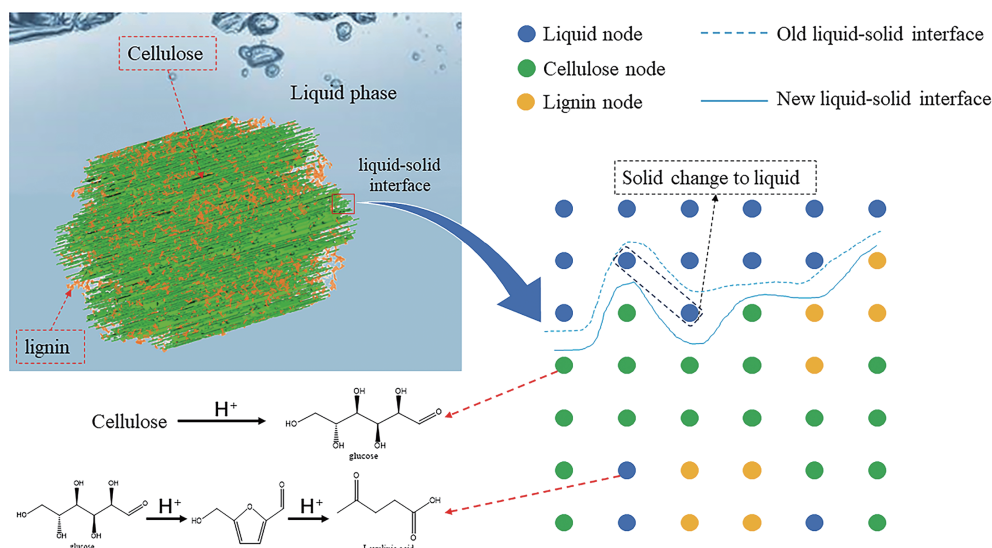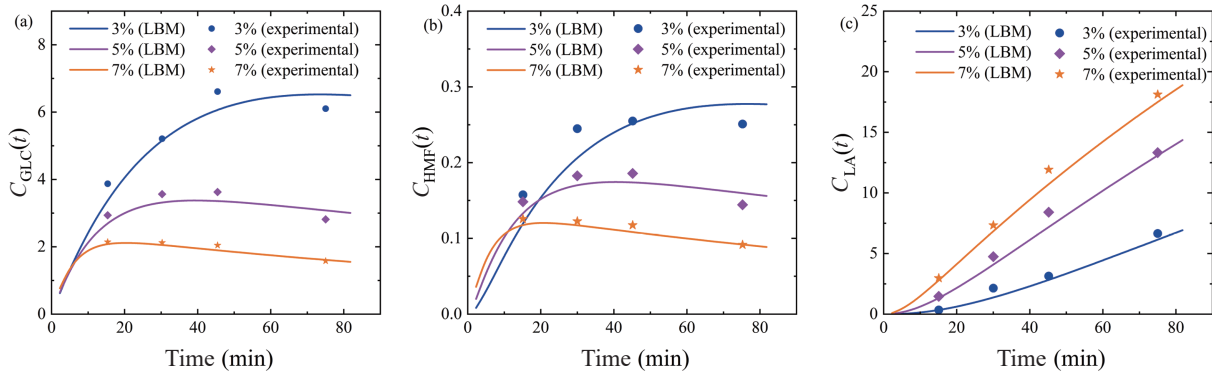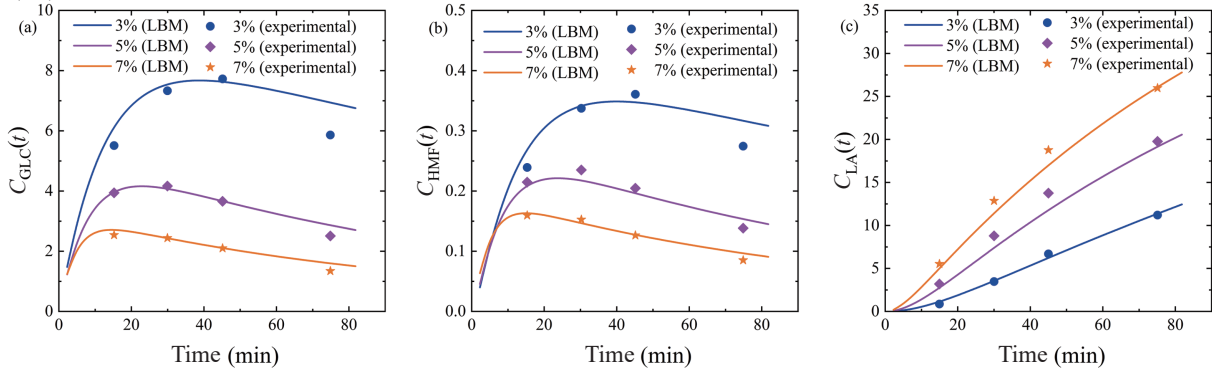

Fig. 2. Schematic of the moving liquid-solid interface.

Fig. 3. Variation of dimensionless concentration curve with reaction time at 150 °C for (a) glucose, (b) 5-hydroxymethylfurfural (HMF), and (c) levulinic acid (LA).

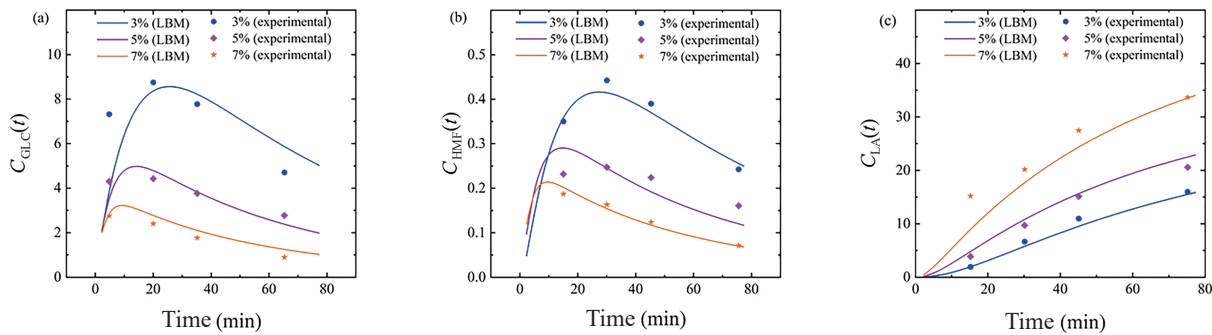
Fig. 4. Variation of dimensionless concentration curve with reaction time at 170 °C for (a) glucose, (b) 5-hydroxymethylfurfural (HMF), and (c) levulinic (LA).

Fig. 5. Variation of dimensionless concentration curve with reaction time at 190 °C for (a) glucose, (b) 5-hydroxymethylfurfural (HMF), and (c) levulinic (LA).

LA in aqueous conditions at 150 – 200 °C, the LA yield decreased with the increase of temperature[16].

Five temperature points were taken between 120 – 200 °C, and the corresponding reaction constants were obtained using the modified Arrhenius formula. The parameters were then added to the LBM to explore the influence of temperature on the conversion of cellulose in solid residue to LA when catalyzed by acid.

Figs. 6 and 7a show that when the temperature exceeds 180 °C, the consumption rate of glucose is very fast to be maintained. When the temperature is low, the hydrolysis rate of cellulose is slow, resulting in a low glucose concentration. When Fig. 7a and Fig.7b were compared, it was observed that the changing trend of HMF concentration was the same as

that of glucose, and the overall difference was one order of magnitude. This is because the reaction rate of HMF is much faster than that of glucose and is almost instantly converted LA. As shown in Fig. 8a, the concentration of LA is the highest when the temperature is 200 °C, but Fig. 8b shows that the increasing rate of LA concentration at 200 °C is slower after 25 min than that at other temperatures.

With the change in temperature, the reaction rate of the side reaction shows a nonlinear change. To investigate the effect of temperature on the hydrolysis reaction and identify the optimum reaction temperature; the conversion rate of glucose, the yield of the final product LA, and the effective yield of carbon were calculated according to Eqs. (22), (23), and (24), respectively:

$$\mathrm{Conv_{GLC}}(t) = \frac{\iiint_{V_{re}} C_{\mathrm{GLC,tot}}(\boldsymbol{x},t)\,\mathrm{d}V - \iiint_{V_{re}} C_{\mathrm{GLC,remain}}(\boldsymbol{x},t)\,\mathrm{d}V}{\iiint_{V_{re}} C_{\mathrm{GLC,tot}}(\boldsymbol{x},t)\,\mathrm{d}V} \times 100\%, \tag{22}$$
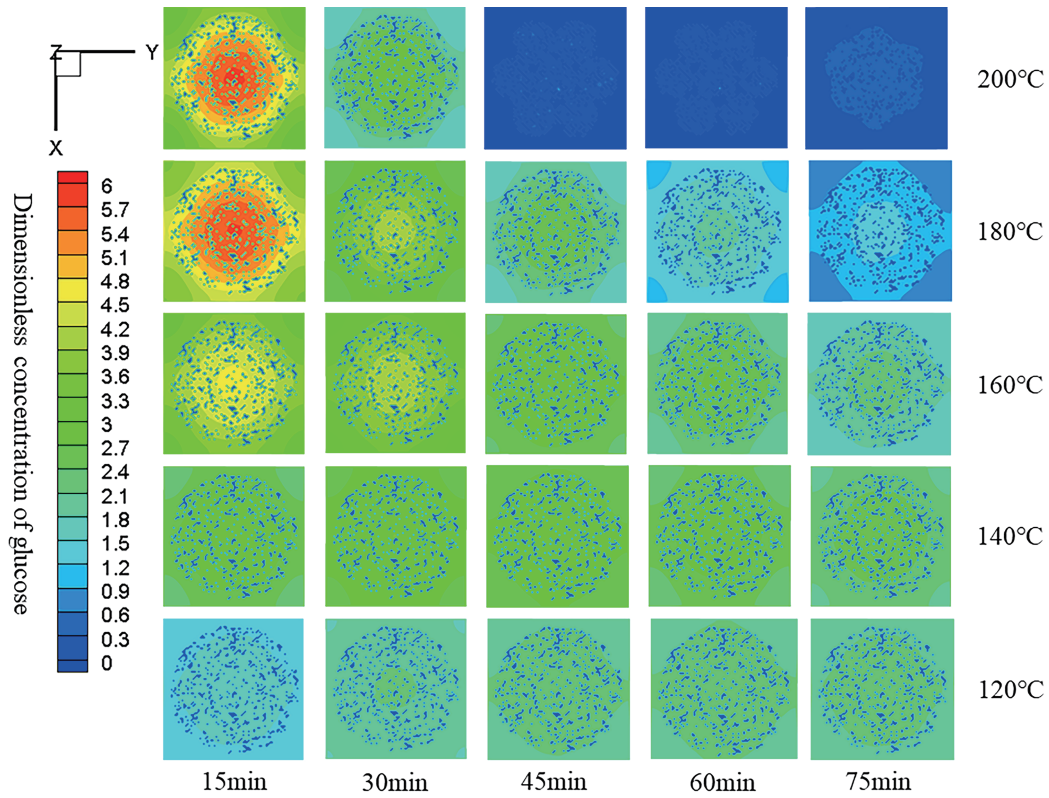
Fig. 6. Contour plots of glucose with dimensionless concentration in the cross-section of the cylinder at different temperatures.
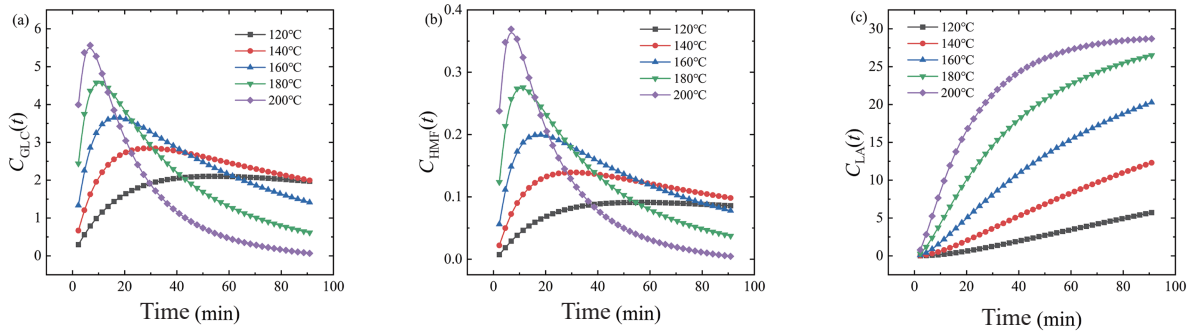

Fig. 7. Time evolution of the dimensionless concentration of (a) glucose, (b) 5-hydroxymethylfurfural (HMF), and (c) levulinic (LA).
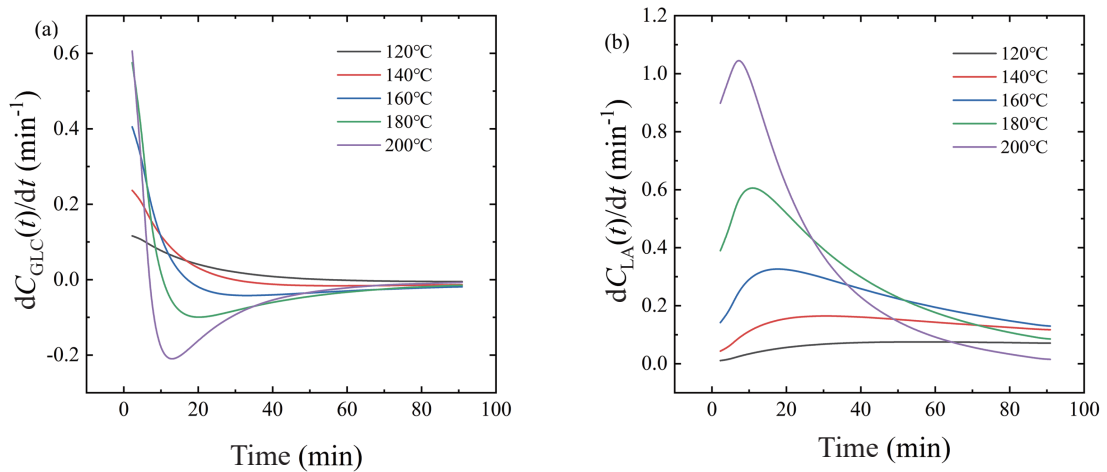

Fig. 8. The overall reaction rate of the product at different temperatures for (a) glucose and (b) levulinic (LA).

$$Y_{LA} = \frac{\iiint_{V_{re}} C_{LA}(\boldsymbol{x},t)\,dV}{\iiint_{V_{re}} C_{GLC,tot}(\boldsymbol{x},t)\,dV} \times 100\%, \qquad (23)$$

$$Y_{carbon}(t) = \frac{\iiint_{V_{re}} C_{LA}(\boldsymbol{x},t)\,dV + \iiint_{V_{re}} C_{HMF}(\boldsymbol{x},t)\,dV}{\iiint_{V_{re}} C_{GLC,tot}(\boldsymbol{x},t)\,dV} \times 100\%, \qquad (24)$$

where $C_{GLC,\,tot}(\boldsymbol{x},\,t)$ is the total concentration of glucose converted from cellulose in the x position from 0 to t; and $C_{GLC,\,remain}(\boldsymbol{x},\,t)$ indicates the concentration of glucose remaining at the x position at t time.

Fig. 9a shows that the conversion rate of glucose is positively related to temperature. The higher the temperature, the faster is the conversion rate which tends to flatten out over time. At 180 °C and 200 °C, the conversion rate of glucose was significantly higher than that at other temperatures. Fig. 9b and c show that at 160 °C, 180 °C, and 200 °C, the efficiency of producing LA is higher than the efficiency at 120 °C and 140 °C. When the temperature exceeds 180 °C, although the increase of temperature increases the hydrolysis rate of cellulose, the rate of formation of humins is also strengthened when glucose is converted to HMF. In comparison, the increase in the rate of LA formation caused by the increase of temperature does not exceed the increase in the rate of the side reaction. Therefore, the highest LA and effective carbon conversion rate is at 180 °C rather than at 200 °C.

3.3 Effect of acid concentration

The effects of different dilute sulfuric acid concentrations on cellulose hydrolysis were evaluated. Assuming that the dilute sulfuric acid concentrations were 4%, 5%, 6%, 7%, and 8%, respectively, and combined with the parameters in Table 1, the reaction rate constants were obtained through the modified Arrhenius formula, and then added to the LBM.

Figs. 10a and 11a show that with an increase in acid concentration, the glucose conversion rate increases, and remaining glucose concentration is low. Figs. 10b and 11b show that the dimensionless concentration of LA increases with the increase of acid concentration, the trend of the LA concentration curve at each concentration is the same, and the final overall reaction rate tends to be equal. Fig. 12a and b show that the simulation results where the dissolution rate of cellulose increases with the increase of acid concentration at the same temperature within the acid concentration range of 4% – 8%.

This was observed mainly because hydrolysis only considers the cellulose hydrolysis and neglects the lignin content in the solid residue. Lignin is not active under the condition of dilute acid catalysis, however, when the temperature reaches 180 °C, it will inevitably agglomerate. Therefore, with higher acid concentration, a part of cellulose will be wrapped and transferred, resulting in a decrease in the conversion and reaction rate of cellulose.

Due to the negligible effect of lignin content in the solid residue, the increase of the reaction rate of the side reaction is
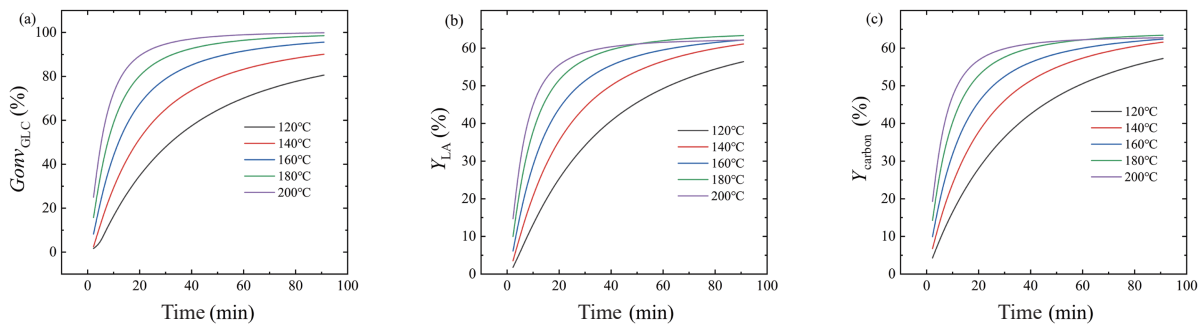

Fig. 9. (a) Conversion rate of glucose, (b) levulinic (LA) yield, and (c) effective carbon yield.
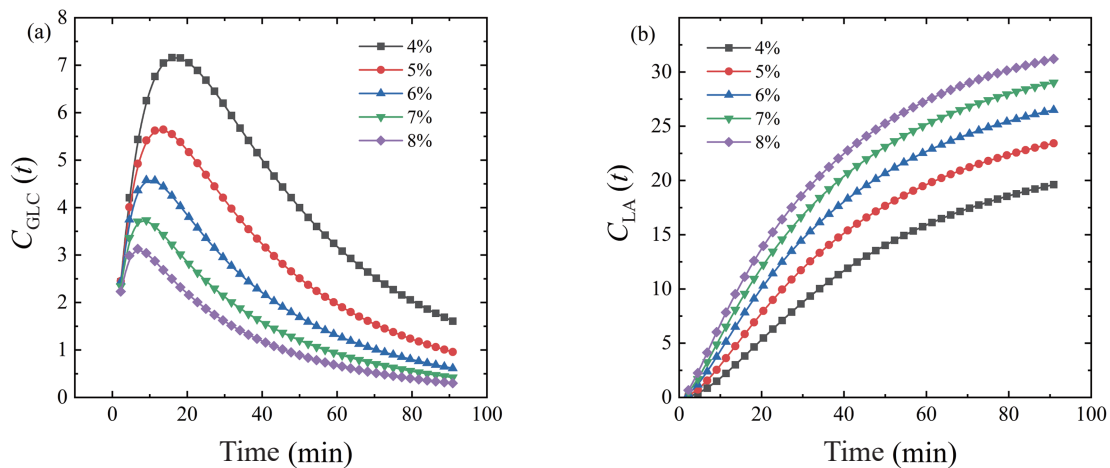

Fig. 10. Time evolution under different acid concentrations of the dimensionless concentration of (a) glucose, and (b) levulinic (LA).
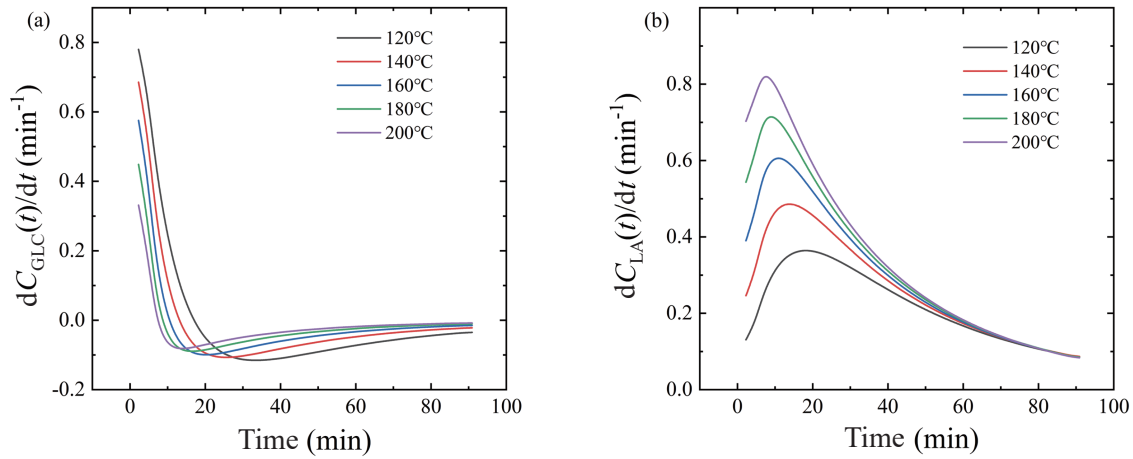
Fig. 11. Time evolution under different acid concentrations of the overall reaction rate of (a) glucose, and (b) levulinic (LA).
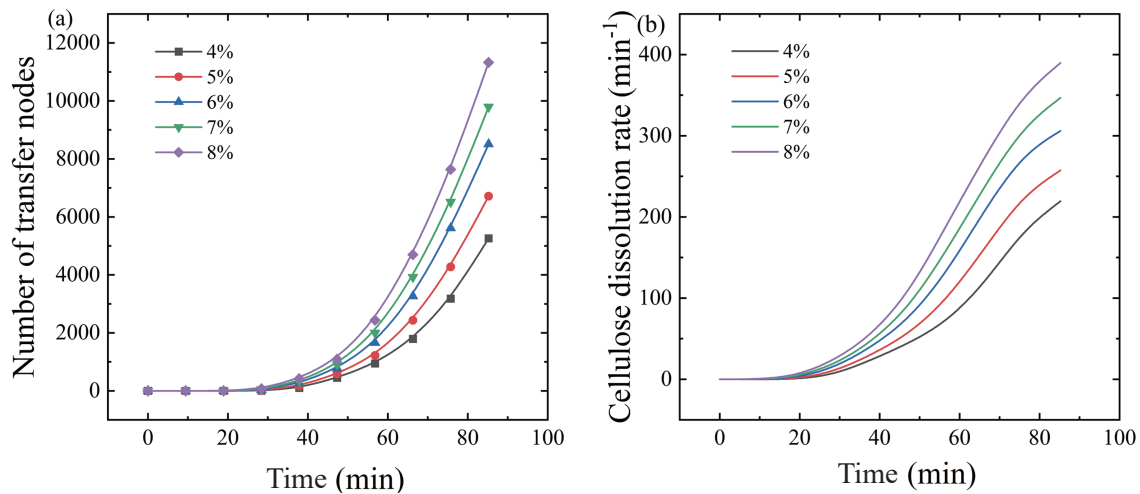

Fig. 12. (a) Time evolution of the number of solid nodes changing to fluid nodes. (b) The dissolution rate of cellulose nodes variation over time.

much lower than that of the main reaction in the acid concentration range of 4% – 8%. The higher the acid concentration, the more efficient is the hydrolysis effect.

3.4 Response characteristics of the hydrolysis performance to the porosity

To explore the performance response of the cellulose hydrolysis reaction to the porosity of the solid residue, the residue structure generation program was modified, and models with porosity of 0.4, 0.5, 0.6, 0.7 and 0.8 were constructed (the pore structure is shown in Fig. 13). Five solid residue structures with different porosity were incorporated into the LBM.

Fig. 14a and b show that when the porosity is lower, the cellulose concentration is higher. The effect of different porosities is apparent, but the trend over time is the same. Fig. 15a shows that when the porosity increases, the rate of conversion of solid cellulose nodes to fluid cellulose nodes is faster, and the average dissolution rate of cellulose is faster. Fig. 15b shows that the dissolution rate of cellulose with a porosity of 0.8 is greatest at the beginning and then decreases. Within 75 min, the average dissolution rate was the highest for cellulose with a porosity of 0.7, but after 75 min, the dissolution rate was the highest for cellulose with a porosity of 0.6.

When the porosity is low, fewer fluid nodes lead to fewer solid nodes for the acid in the fluid to interact with, which results in the slower dissolution of cellulose. As the porosity increases, the possibility that there is a fluid node around the
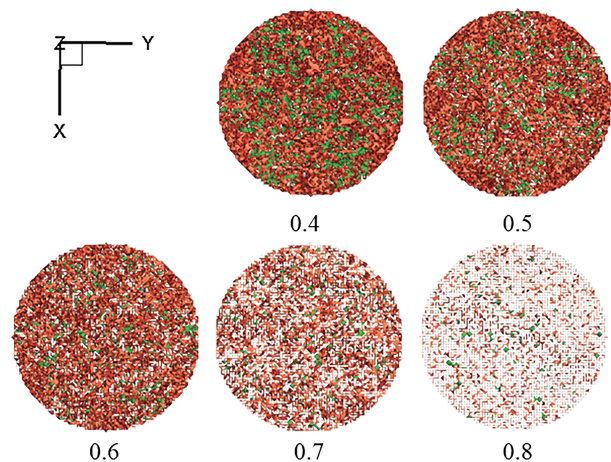

Fig. 13. Schematic diagram of the structure of porous media along the axial direction of a cylinder under different porosity values. The green part is cellulose, and the orange part is lignin.
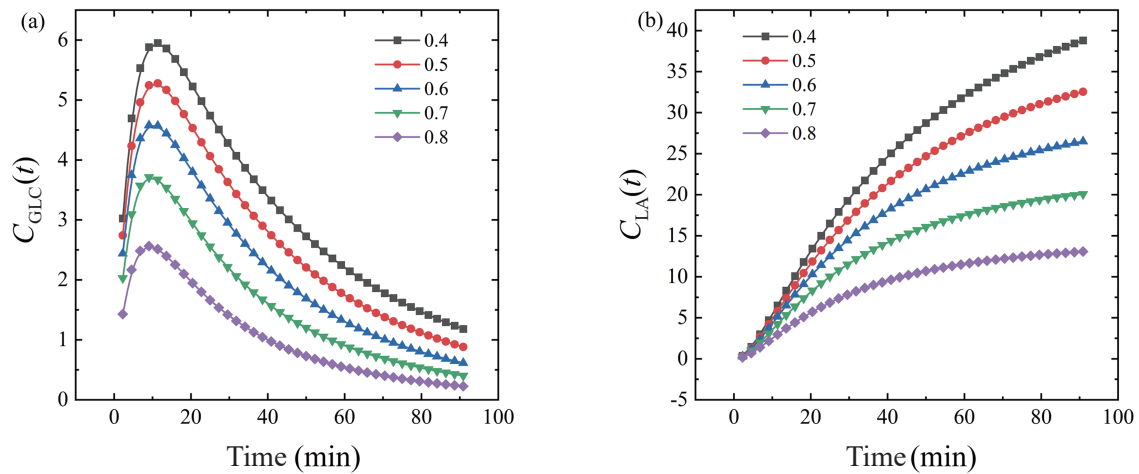
Fig. 14. Time evolution under different porosities of the dimensionless concentration of (a) glucose, and (b) levulinic (LA).
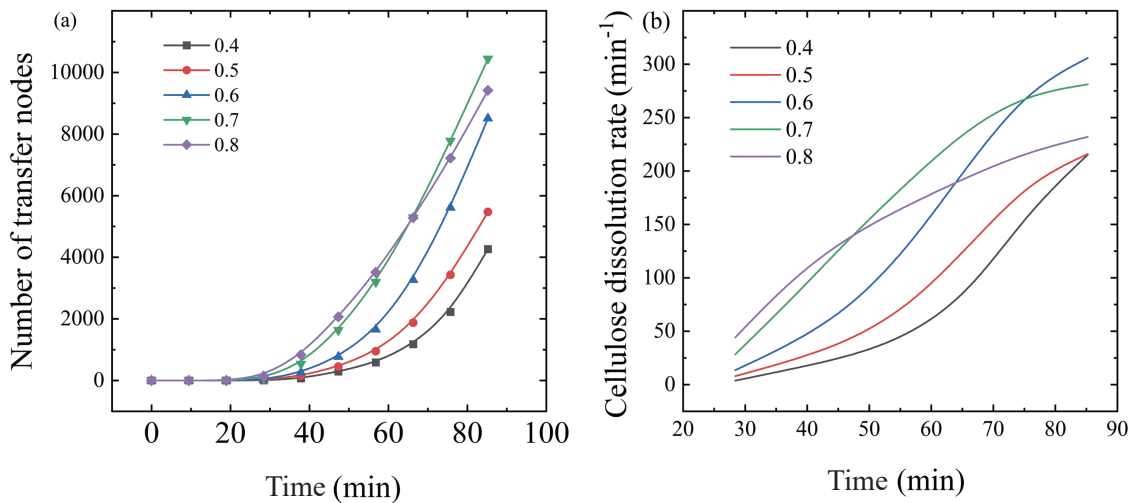

Fig. 15. (a) The number of solid nodes changing to fluid nodes varies with time under different porosities. (b) The dissolution rate of cellulose nodes over time.

cellulose node becomes greater, therefore the dissolution of cellulose is accelerated. However, when the porosity is large, although there are more fluid nodes, the number of solid cellulose nodes that act as substrates is low. Therefore, fewer cellulose nodes are in contact with the fluid nodes. When the reaction has progressed to a certain extent, the dissolution of cellulose leads to an increase in the overall porosity of the model with low initial porosity, which increases the contact between the cellulose nodes and the dilute acid catalyst.

3.5 The effect of cellulose proportion

The content of cellulose varies for different biomass raw materials. Therefore, this section focuses on the influence of varying cellulose proportions on the effect of hydrolysis. By adjusting the residue structure generation program, assuming that the hydrolysis temperature is 180 °C, the acid concentration is 6%, and the overall porosity is 0.6, and varying the proportion of cellulose from 40%, 50%, 60%, and 70%, the four different residue structures were examined in the LBM.

As shown in Fig. 16a and b, when the proportion of cellulose increases from 40% to 70%, the concentration of glucose and LA increases at the same time, and the trend is the

same over time for materials with different cellulose contents. However, in Fig. 17a the number of solid nodes to fluid nodes is not positively related to the cellulose content. Fig. 17a and b show that within 75 min the model with the cellulose content of 50% has a higher average cellulose dissolution rate than the others.

For a set porosity, when the cellulose proportion of the solid content is relatively large, the cellulose aggregates. As a result, the dilute acid in the fluid needs to dissolve the outer layer of cellulose before the hydrolysis reaction can commence. When the cellulose proportion is lower, its distribution is more uniform and the degree of aggregation decreases, and the cellulose interfaces with the fluid nodes more efficiently. However, when the cellulose proportion is less than 50%, fewer total cellulose nodes result in fewer cellulose nodes in contact with fluid nodes which leads to a lower dissolution rate.

Fig. 17b shows that simulations with initial cellulose content higher than 50% had greater cellulose dissolution rates than simulations with initial cellulose content of 50% after 75 min as the cellulose nodes were in complete contact with the fluid nodes.
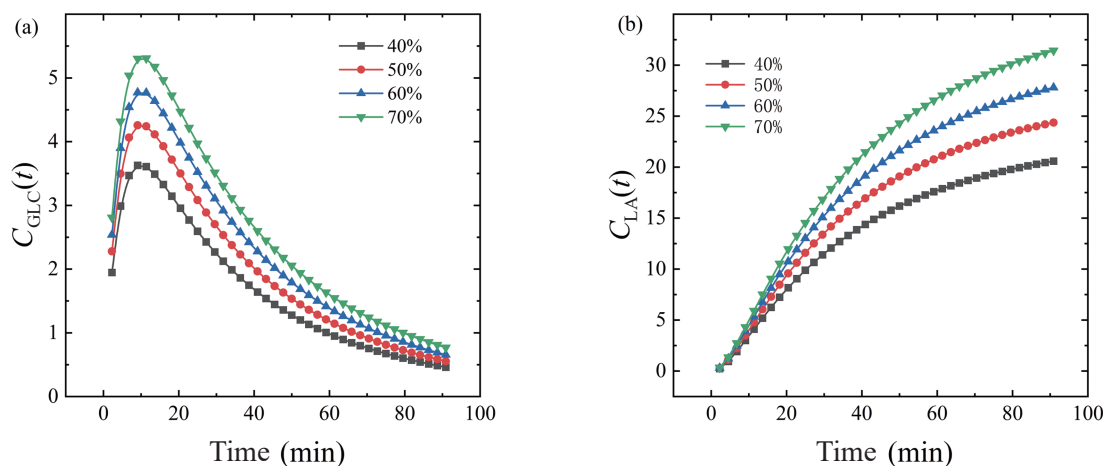
Fig. 16. Time evolution under different cellulose contents of the dimensionless concentration of (a) glucose, and (b) levulinic (LA).
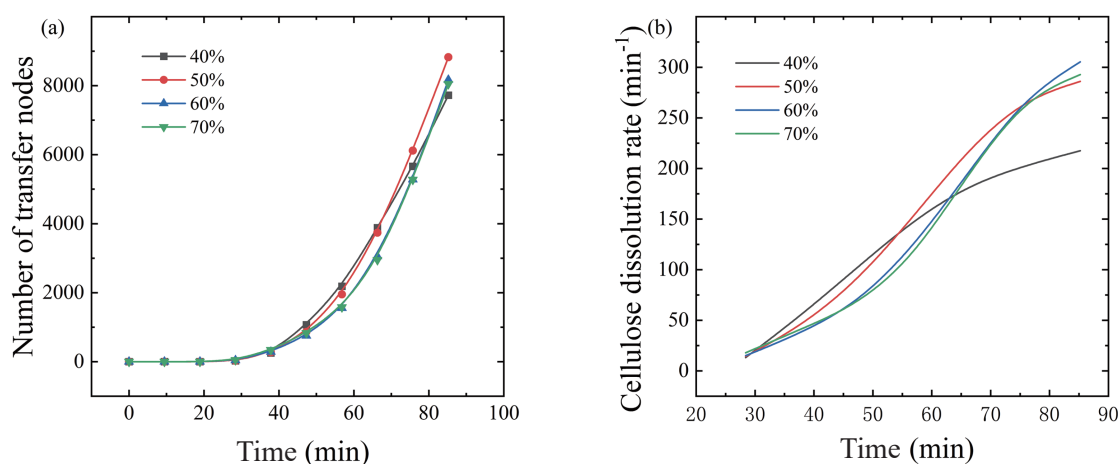

Fig. 17. (a) The number of solid nodes changing to fluid nodes over time for different cellulose contents. (b) The dissolution rate of cellulose over time.

4 Conclusions

In this study, a multiphase reactive transport model for the extraction of LA from lignocellulose biomass residue catalyzed by dilute acid was established based on the LBM. The study of the complex physicochemical mechanism in this process identified the improvements for the hydrolysis rate of cellulose and the effect of acid-catalyzed hydrolysis. The proposed model considers the transport of porous media in solid residue, multi-component transport in solution, liquid-solid interface reaction, hydrogen ion catalysis in solution, solid dissolution of cellulose, and the structural evolution of porous solid residue. The dimensionless concentrations of glucose, HMF, and LA predicted by the simulation were correlated with the experimental results. The effects of different temperatures, acid concentrations, solid residue porosities, and cellulose contents in the residue on the hydrolysis performance were also evaluated. The main conclusions of this study are as follows:

(I) Between 120 – 200 °C, the overall reaction rate was faster as the temperature increased. For temperatures higher than 180 °C, the increase of the side reaction rate was higher than that of the main reaction, resulting in a decrease in the yield of the final LA product. Therefore, the highest effective

yield of carbon was obtained at 180 °C.

(II) When the effects of lignin were ignored, the increase in the side reaction rate caused by the increase in acid concentration was much lower than the increase in the rate of the main reaction. Therefore, the higher the acid concentration, the faster is the hydrolysis rate of the solid residue and the higher the LA yield.

(III) Under the same reaction conditions, the lower the porosity, the higher is the concentration of the product. However, low porosity may decrease the accessibility of the cellulose solid nodes which leads to the decrease of the overall cellulose dissolution rate. However, when the porosity is very large, the overall dissolution rate decreases because the number of available cellulose nodes is very low. Therefore, the increase of overall porosity due to the dissolution of cellulose, leads to a higher dissolution rate of the model with lower initial porosity. Between 45 and 75 min, when the porosity is 0.7, the average dissolution rate of cellulose is the fastest.

(IV) Under the same reaction conditions and porosity, with the increase in the content of cellulose, the concentration of the products increase. During the initial period of the reaction, when the cellulose proportion exceeds 50%, the overall dissolution rate of cellulose due to cellulose agglomeration is

lower than that when the cellulose proportion is 50%. When the cellulose proportion is less than 50%, the overall dissolution rate decreases because there is very little cellulose. Within 75 min, when the cellulose content is 50%, the average dissolution rate of cellulose is the fastest. For cases where the initial cellulose content is higher than 50%, when the reaction time exceeds 75 min, the increase in porosity caused by the dissolution of cellulose will increase the dissolution rate of cellulose.

In this study, the lattice Boltzmann method was used to explore the hydrolysis of cellulose in solid residues to form levulinic acid for the first time, which provided a theoretical basis for optimizing the performance of the hydrolysis reaction. But in order to simplify the model, the influence of lignin in the residue and the coking phenomenon that might be caused by side reactions were not considered in this study.

Acknowledgements

Conflict of interest

The authors declare that they have no conflict of interest.

Biographies

Haoyang Wei is currently pursuing a master's degree at the University of Science and Technology of China. His research focuses mainly on numerical simulation of biomass hydrothermal conversion.

Chengguang Wang received his Ph.D. degree in Thermal Engineering from Guangzhou Institute of Energy Conversion (GIEC), Chinese Academy of Sciences in 2009. He joined GIEC in 2013 and is now the director of Biomass Catalytic Conversion Laboratory. His research interests include fundamental and applied research in biomass catalytic conversion to aviation fuel and high value chemicals.

Longlong Ma received his Ph.D. degree from East China University of Science and Technology in 2007. From 2002 to 2021, he worked in Guangzhou Institute of Energy Research, Chinese Academy of Sciences, and served successively as researcher, deputy director, party secretary and director. He is currently a professor at the School of Energy and Environment, Southeast University. His research interests include the theory studies on the aqueous catalysis of biomass; biomass pyrolysis, gasification and power generation; efficient conversion and application of biomass.

References

[1] Ragauskas A J, Williams C K, Davison B H, et al. The path forward for biofuels and biomaterials. *Science,* **2006**, *311* (5760): 484–489.

[2] Takagaki A, Nishimura S, Ebitani K. Catalytic transformations of biomass-derived materials into value-added chemicals. *Catalysis Surveys from Asia,* **2012**, *16* (3): 164–182.

[3] Alonso D M, Hakim S H, Zhou S, et al. Increasing the revenue from lignocellulosic biomass: Maximizing feedstock utilization. *Science Advances,* **2017**, *3* (5): e1603301.

[4] Climent M J, Corma A, Iborra S. Conversion of biomass platform molecules into fuel additives and liquid hydrocarbon fuels. *Green Chemistry,* **2014**, *16* (2): 516–547.

[5] Isikgor F H, Becer C R. Lignocellulosic biomass: a sustainable platform for the production of bio-based chemicals and polymers. *Polymer Chemistry,* **2015**, *6* (25): 4497–4559.

[6] Pileidis F D, Titirici M M. Levulinic acid biorefineries: New challenges for efficient utilization of biomass. *ChemSusChem,* **2016**, *9* (6): 562–582.

[7] Yan K, Jarvis C, Gu J, et al. Production and catalytic transformation of levulinic acid: A platform for speciality chemicals and fuels. *Renewable and Sustainable Energy Reviews,* **2015**, *51*: 986–997.

[8] Huber G W, Iborra S, Corma A. Synthesis of transportation fuels from biomass: Chemistry, catalysts, and engineering. *Chemical Reviews,* **2006**, *106* (9): 4044–4098.

[9] Van Buijtenen J, Lange J P, Alonso L E, et al. Furfural production by 'acidic steam stripping' of lignocellulose. *ChemSusChem,* **2013**, *6* (11): 2132–2136.

[10] Shinde S D, Meng X, Kumar R, et al. Recent advances in understanding the pseudo-lignin formation in a lignocellulosic biorefinery. *Green Chemistry,* **2018**, *20* (10): 2192–2205.

[11] Ruiz H A, Conrad M, Sun S N, et al. Engineering aspects of hydrothermal pretreatment: From batch to continuous operation, scale-up and pilot reactor under biorefinery concept. *Bioresource Technology,* **2020**, *299*: 122685.

[12] Li Y, Zhao C, Chen L, et al. Production of bio-jet fuel from corncob by hydrothermal decomposition and catalytic hydrogenation: Lab analysis of process and techno-economics of a pilot-scale facility. *Applied Energy,* **2018**, *227*: 128–136.

[13] Camacho F, González-Tello P, Jurado E, et al. Microcrystalline-cellulose hydrolysis with concentrated sulphuric acid. *Journal of Chemical Technology & Biotechnology,* **1996**, *67* (4): 350–356.

[14] Kim J S, Lee Y Y, Torget R W. Cellulose hydrolysis under extremely low sulfuric acid and high-temperature conditions. *Applied Biochemistry and Biotechnology,* **2001**, *91* (1): 331–340.

[15] Mosier N S, Sarikaya A, Ladisch C M, et al. Characterization of dicarboxylic acids for cellulose hydrolysis. *Biotechnology Progress,* **2001**, *17* (3): 474–480.

[16] Girisuta B, Janssen L P B M, Heeres H J. Kinetic study on the acid-catalyzed hydrolysis of cellulose to levulinic acid. *Industrial & Engineering Chemistry Research,* **2007**, *46* (6): 1696–1708.

[17] Patil S K R, Heltzel J, Lund C R F. Comparison of structural features of humins formed catalytically from glucose, fructose, and 5-hydroxymethylfurfuraldehyde. *Energy Fuels,* **2012**, *26* (8): 5281–5293.

[18] Jing Q, Lü X. Kinetics of non-catalyzed decomposition of glucose in high-temperature liquid water. *Chinese Journal of Chemical Engineering,* **2008**, *16* (6): 890–894.

[19] Li Q, Luo K H, Kang Q J, et al. Lattice Boltzmann methods for multiphase flow and phase-change heat transfer. *Progress in Energy and Combustion Science,* **2016**, *52*: 62–105.

[20] Van den Akker H E A. Lattice Boltzmann simulations for multi-scale chemical engineering. *Current Opinion in Chemical Engineering,* **2018**, *21*: 67–75.

[21] Zhu J, Ma J. An improved gray lattice Boltzmann model for simulating fluid flow in multi-scale porous media. *Advances in Water Resources,* **2013**, *56*: 61–76.

[22] Xu A, Shi L, Xi H D. Lattice Boltzmann simulations of three-dimensional thermal convective flows at high Rayleigh number. *International Journal of Heat and Mass Transfer,* **2019**, *140*: 359–370.

[23] Li D, Ren Q, Tong Z X, et al. Lattice Boltzmann models for axisymmetric solid–liquid phase change. *International Journal of Heat and Mass Transfer,* **2017**, *112*: 795–804.

[24] Nemati M, Shateri Najaf Abady A R, Toghraie D, et al. Numerical investigation of the pseudopotential lattice Boltzmann modeling of liquid–vapor for multi-phase flows. *Physica A: Statistical Mechanics and its Applications,* **2018**, *489*: 65–77.

[25] Liu H, Kang Q, Leonardi C R, et al. Multiphase lattice Boltzmann simulations for porous media applications. *Computational Geosciences,* **2016**, *20* (4): 777–805.

[26] Liu M, Mostaghimi P. High-resolution pore-scale simulation of dissolution in porous media. *Chemical Engineering Science,* **2017**, *161*: 360–369.

[27] Falcucci G, Amati G, Krastev V K, et al. Heterogeneous catalysis in pulsed-flow reactors with nanoporous gold hollow spheres. *Chemical Engineering Science,* **2017**, *166*: 274–282.

[28] Liu S, Wei X, Sun W, et al. Coking prediction in catalytic glucose conversion to levulinic acid using improved lattice Boltzmann model. *Industrial & Engineering Chemistry Research,* **2020**, *59* (39): 17462–17475.

[29] Shan X, Chen H. Lattice Boltzmann model for simulating flows with multiple phases and components. *Physical Review E,* **1993**, *47* (3): 1815–1819.

[30] Pan C, Hilpert M, Miller C T. Lattice-Boltzmann simulation of two-phase flow in porous media. *Water Resources Research,* **2004**, *40* (1): W01501.

[31] Mei Q, Wei X, Sun W, et al. Liquid membrane catalytic model of hydrolyzing cellulose into 5-hydroxymethylfurfural based on the lattice Boltzmann method. *RSC Advances,* **2019**, *9* (23): 12846–12853.

[32] Yuan P, Schaefer L. Equations of state in a lattice Boltzmann model. *Physics of Fluids,* **2006**, *18* (4): 042101.

[33] Wei X, Li W, Liu Q, et al. Pore-scale investigation on multiphase reactive transport for the conversion of levulinic acid to γ-valerolactone with Ru/C catalyst. *Chemical Engineering Journal,* **2022**, *427*: 130917.

[34] Yu Z, Fan L S. Multirelaxation-time interaction-potential-based lattice Boltzmann model for two-phase flow. *Physical Review E,* **2010**, *82* (4): 046708.

[35] Wang M, Wang J, Pan N, et al. Mesoscopic predictions of the effective thermal conductivity for microscale random porous media. *Physical Review E,* **2007**, *75* (3): 036702.

[36] Lopes E S, Rivera E C, de Jesus Gariboti J C, et al. Kinetic insights into the lignocellulosic biomass-based levulinic acid production by a mechanistic model. *Cellulose,* **2020**, *27* (10): 5641–5663.

[37] Petridis L, Smith J C. Molecular-level driving forces in lignocellulosic biomass deconstruction for bioenergy. *Nature Reviews Chemistry,* **2018**, *2* (11): 382–389.

[38] Shen X, Sun R. Recent advances in lignocellulose prior-fractionation for biomaterials, biochemicals, and bioenergy. *Carbohydrate Polymers,* **2021**, *261*: 117884.

[39] Chen L, Kang Q, Robinson B A, et al. Pore-scale modeling of multiphase reactive transport with phase transitions and dissolution-precipitation processes in closed systems. *Physical Review E,* **2013**, *87* (4): 043306.

[40] Chen L, Kang Q, Tang Q, et al. Pore-scale simulation of multicomponent multiphase reactive transport with dissolution and precipitation. *International Journal of Heat and Mass Transfer,* **2015**, *85*: 935–949.

[41] Chen L, Wang M, Kang Q, et al. Pore scale study of multiphase multicomponent reactive transport during CO_2 dissolution trapping. *Advances in Water Resources,* **2018**, *116*: 208–218.

[42] Ma C, Cai B, Zhang L, et al. Acid-catalyzed conversion of cellulose into levulinic acid with biphasic solvent system. *Frontiers in Plant Science,* **2021**, *12*: 630807.

[43] Weingarten R, Conner W C, Huber G W. Production of levulinic acid from cellulose by hydrothermal decomposition combined with aqueous phase dehydration with a solid acid catalyst. *Energy & Environmental Science,* **2012**, *5* (6): 7559–7574.